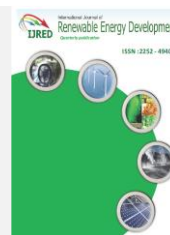




Contents list available at IJRED website

**International Journal of Renewable Energy Development**

Journal homepage: <https://ijred.undip.ac.id>



Research Article

## Removal efficiency and reaction kinetics of phenolic compounds in refinery wastewater by nano catalytic wet oxidation

Yousif S. Issa<sup>1</sup>, Khaleel I. Hamad<sup>2</sup>, Rafi J. Algawi<sup>1</sup>, Jasim I. Humadi<sup>1\*</sup>, Sara Al-Salihi<sup>3</sup>,  
Mustafa A. Ahmed<sup>4</sup>, Ahmed A. Hassan<sup>5</sup>, Abdul-Kareem Abd Jasim<sup>6</sup>

<sup>1</sup> Department of Petroleum and Gas Refining Engineering, College of Petroleum Processes Engineering, Tikrit University, Iraq

<sup>2</sup> Slah Al-Deen, General Directorate of Education, Iraq

<sup>3</sup> Department of Biomedical, Biological & Chemical Engineering, University of Missouri, Columbia, 65211, United States

<sup>4</sup> Ministry of Oil, Baghdad, Iraq

<sup>5</sup> North Refineries Company, Baji Refineries, Ministry of Oil, Iraq

<sup>6</sup> Oil Products Distribution Company, Salahaddin Branch Ministry of Oil, Iraq

**Abstract.** A novel nano-catalyst based on iron oxide ( $\text{MnO}_2/\text{Fe}_2\text{O}_3$ ) was developed to promote wet oxidation of phenol.  $\text{MnO}_2$  was doped in  $\text{Fe}_2\text{O}_3$  matrix to prepare composite nano-catalyst with different doping percentage (0, 2 and 5%). The catalytic phenol oxidation was conducted under different reaction temperatures and residence times. To evaluate the optimal kinetic parameters aiming to maximize phenol removal under the optimal conditions for the catalytic wet phenol oxidation process, modeling was applied on the batch reactor using the novel synthesis nano-catalyst ( $\text{MnO}_2/\text{Fe}_2\text{O}_3$ ) and the model developed was fed with the experimental data. gPROMS package was used to model the process of phenol oxidation and to optimize the experimental data. The error predicted between the simulated and experimental data was less than 5%. The optimal operating conditions were 294 min residence time, 70°C reaction temperature, and 764 ppm initial concentration of phenol over the prepared 5%  $\text{MnO}_2/\text{Fe}_2\text{O}_3$ . Running of wet oxidation of phenol under the optimal operating conditions resulted in 98% removal of phenol from refinery wastewater.

**Keywords:** Nano-catalyst; manganese oxide/ iron oxide; phenol; oxidation process; optimization



@ The author(s). Published by CBIORE. This is an open access article under the CC BY-SA license (<http://creativecommons.org/licenses/by-sa/4.0/>).

Received: 24<sup>th</sup> January 2023; Revised: 5<sup>th</sup> March 2023; Accepted: 30<sup>th</sup> March 2023; Available online: 11<sup>th</sup> April 2023

### 1. Introduction

The water contamination by organic compounds is considered as a threat to the health of human and overall quality of water since the wastewater is predominating released from industrial plants without any efficient treatment. Phenol and phenolic compounds are considered a priority pollutant contaminant categorized as teratogenicity and carcinogenic (Saravanan *et al.*, 2021; Stefanakis & Thullner, 2016; Wang, Bian, & Li, 2012; Yaqub, Isa, Ajab, & Junaid, 2017). Different technologies, such as electrochemical degradation (Iniesta, González-García, Exposito, Montiel, & Aldaz, 2001; Li, Cui, Feng, Xie, & Gu, 2005; Luo, Li, Wu, Zheng, & Dong, 2015), biodegradation (Amor, Eiroa, Kennes, & Veiga, 2005; Kumar, Kumar, & Kumar, 2005; Peyton, Wilson, & Yonge, 2002), physical sorption (Hamad *et al.*, 2022b; Humadi *et al.*, 2022; Li *et al.*, 2002; Pan *et al.*, 2003), and the advanced oxidation Processes (AOPs) (Amor *et al.*, 2019; Aziz, Asaithambi, & Daud, 2016; Esplugas, Gimenez, Contreras, Pascual, & Rodríguez, 2002; Hamad *et al.*, 2022b; Martins & Quinta-Ferreira, 2011; Xu, Siracusa, Di Gregorio, & Yuan, 2018) have been employed to purify the wastewater. The advanced oxidation processes (AOPs) are characterized by producing highly reactive oxidizing radicals, can degrade these organic

contaminants to carbon dioxide, water, and mineral salts (mineralization) (Covinich, Bengoechea, Fenoglio, & Area, 2014; Gagol *et al.*, 2020; Lozano, Devard, Ulla, & Zamaro, 2020; Shahidi, Roy, & Azzouz, 2015). AOPs processes include treatment with UV/ $\text{H}_2\text{O}_2$ , ozonation, photocatalysis, air wet oxidation and catalytic wet peroxide oxidation (CWPO). Hydrogen peroxide ( $\text{H}_2\text{O}_2$ ) is a green oxidant has the ability to work in the CWPO at moderate operating conditions (atmospheric pressure,  $T < 80^\circ\text{C}$ ) (Busca, Berardinelli, Resini, & Arrighi, 2008; Martin-Martinez *et al.*, 2016; Piccinin, 2022; Shahidi *et al.*, 2015). Also, hydrogen peroxide is utilized as liquid oxidant in CWPO to overcome the gas-liquid mass transfer limitations and significantly enhance the efficiency of process. CWPO is superior to other AOPs technologies because it provides lower activation energy by utilizing a catalyst to enable the reaction to proceed under mild operating conditions (Baloyi, Ntho, & Moma, 2018; Wang *et al.*, 2021; Yan, Wu, & Zhang, 2016). Recently, there is a growing attention in the use of iron oxide nanoparticles for the removal of heavy metal found in wastewater owing to their availability and simplicity. In general, due to the small size of Nano sorbent materials, their separation and recovery from contaminated water is an important issue for

\* Corresponding author

Email: [jasim\\_alhashimi\\_ppe@tu.edu.iq](mailto:jasim_alhashimi_ppe@tu.edu.iq) (J.I.Humadi)

water purification. The application of  $\text{Fe}_2\text{O}_3$  nanoparticles as catalysts in organic synthesis is a large field and has become the focus of research community in recent years.  $\text{Fe}_2\text{O}_3$  nanoparticles have interesting physical and chemical properties that are quite different from their corresponding bulk phases, which make them very efficient catalysts for a variety of reactions. Efficient distribution of the catalyst in the reaction medium, large surface area of the particles, and easy recovery by magnetic separation are some of the benefits of using these materials.  $\text{Fe}_2\text{O}_3$  nanoparticles are considered as a promising catalyst for oxidation reactions of different organic compounds (Ahmed, El-Katori, & Gharni, 2013; Khasawneh & Palaniandy, 2021; Lokhat, Oliver, & Carsky, 2015). Manganese oxide ( $\text{MnO}_2$ ) is an important catalyst or oxidant in the natural environment, which can efficiently degrade a variety of organic pollutants. Manganese oxides have diverse catalytic uses due to their extremely efficient redox properties, and the mixed valences have been emphasized as essential in redox catalysis as well as electron and energy transfer (Fei *et al.*, 2017; Hu *et al.*, 2019).

In this study, the catalytic oxidation of phenol was carried out  $\text{H}_2\text{O}_2$  as an oxidant in the presence of a novel nano-catalyst composite ( $\text{MnO}_2/\text{Fe}_2\text{O}_3$ ) under mild operating conditions. To scaling up and zero emission, the experimental results were used to optimize the kinetic parameters and to produce the optimal operating conditions of the process.

## 2. Experimental work

### 2.1 Materials

In this work, the feedstock was prepared by adding the desired initial phenol concentration (supplied by Alpha Chemika Company, ~99% pure) to demineralized water. The oxidant used in the oxidation process was hydrogen peroxide ( $\text{H}_2\text{O}_2$ ) obtained from (Merck Millipore Company, Germany) with a purity of 31.0 %.

### 2.2 Catalyst preparation

The materials used to prepare the nano-catalyst ( $\text{MnO}_2/\text{Fe}_2\text{O}_3$ ) were Manganese (II) chloride ( $\text{MnCl}_2 \cdot 4\text{H}_2\text{O}$ , 98%, (Thomas Baker), Iron oxide ( $\text{Fe}_2\text{O}_3$ , 98%, (Sky spring)), and deionized water. Manganese oxide was loaded over the catalyst support (iron oxide) via wet impregnation method. A desired quantity of  $\text{MnCl}_2 \cdot 4\text{H}_2\text{O}$  salt was dissolved in deionized water, to obtain the precursor salt solution. Then,  $\text{Fe}_2\text{O}_3$  was gradually added to the prepared salt solution with stirring. The impregnated solution was heated by oven to 120 °C for overnight and then calcined in a furnace at 550 °C for 4 h at a heating ramp of 10 °C/min. The samples were left overnight to cool to room temperature.

### 2.3 Catalyst evaluation

The conditions used to catalyze the phenol oxidation process are shown in Table 1. The prepared catalysts ( $\text{MnO}_2/\text{Fe}_2\text{O}_3$ ) were evaluated for oxidation of phenol in the simulated refinery wastewater (initial phenol concentration = 634 ppm) in a 3-neck

**Table 1**

Operating conditions for catalytic phenol oxidation processes

Operating parameter	Value
Type of catalyst	CAT-1= $\text{Fe}_2\text{O}_3$ CAT-2= 2% $\text{MnO}_2/\text{Fe}_2\text{O}_3$ CAT-3= 5% $\text{MnO}_2/\text{Fe}_2\text{O}_3$
Reaction temperature, °C	30, 45, 60, 75
Residence time, min	20, 40, 60, 80, 100, 120
$\text{H}_2\text{O}_2$ , M	1
Pressure, atm	1

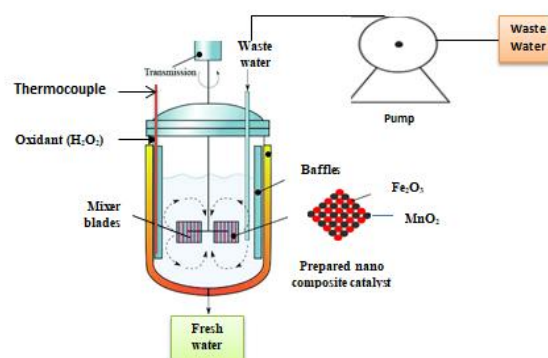


**Fig 1.** Experimental setup for the catalytic wet phenol oxidation process.

glass batch reactor connected to a condenser and temperature controller. In all experiments, the prepared catalyst (1 g) was added after the wastewater reached the desired reaction temperature. Then, the  $\text{H}_2\text{O}_2$  solution was added to the catalyst-phenol solution. After each oxidation reaction run, the reaction mixture was cooled to room temperature and the catalyst was separated from the oxidant-phenol solution by filtration. Figure 1 was showed the experimental setup for the catalytic wet phenol oxidation process.

## 3. Mathematical model of batch reactor for catalytic phenol oxidation reaction

A mathematical model of the catalytic phenol oxidation process was developed in the gPROMS program (Pan *et al.*, 2003). (General Process Modeling System, Version 7.07 (2021, License ref: 27552) is officially licensed to Tikrit University by Siemens AG, UK). The equations used in the mathematical modeling are summarized in Table 2.

## 4. Evaluation of kinetic parameters

### 4.1 Constant parameters for determining of kinetic parameters

The optimal kinetic parameters of the catalytic phenol oxidation were specified by applying mathematical modeling technique that minimized the error between the concentrations of phenol produced by experimental runs and values determined by the model. The constant parameters applied in the mathematical modeling technique are summarized in Table 3.

### 4.2 Kinetic parameters estimation technique using process modeling

To evaluate appropriate values of kinetic parameters for catalytic phenol oxidation, the following objective function must be minimized, as follows:

$$OBJ = \sum_{n=1}^{Nt} (C_{phenol}^{exp} - C_{phenol}^{pred})^2 \quad (18)$$

In equation (18),  $C_{phenol}^{exp}$ ,  $C_{phenol}^{prd}$  and  $Nt$  represent the final phenol content obtained from the experimental run, the final phenol content evaluated by the mathematical model, and the number of experimental runs, respectively. The amount of phenol degradation was estimated by using the following equation (19):

**Table 2**  
Equations used in mathematical modeling

Parameter (Symbol)	Equations/values	Eq. no.	Ref.
Rate of reaction ( $-r_{ph}$ )	$(-r_{ph}) = \eta_0 k C_{ph}^n$	(1)	(Hamad <i>et al.</i> , 2022a; Humadi <i>et al.</i> , 2023; Humadi <i>et al.</i> , 2022)
Arrhenius equation ( $k$ )	$k = k_0 e^{(-\frac{EA}{RT})}$	(2)	(Huang, Luo, Kang, Zhu, & Dai, 2017; Humadi <i>et al.</i> , 2023; Saha, Kumar, & Sengupta, 2019)
The final phenol content ( $C_{ph}$ )	$C_{ph} = [C_{ph,t}^{(1-n)} + (n-1) \cdot t \cdot K_{in} \eta_0]^{\frac{1}{1-n}}$	(3)	
The effectiveness factor ( $\eta_0$ )	$\eta_0 = \frac{3(\phi \coth \phi - 1)}{\phi^2}$	(4)	(Esplugas <i>et al.</i> , 2002)
Thiele modulus ( $\phi$ )	$\phi = \frac{V_p}{S_p} \sqrt{\left(\frac{n+1}{2}\right) \frac{k_{in} C_{ph}^{(n-1)} \rho_p}{D_{ei}}}$	(5)	(Humadi <i>et al.</i> , 2022)
The catalyst effective diffusivity ( $D_{ei}$ )	$D_{ei} = \frac{\epsilon_B}{\mathcal{T}} \frac{1}{\frac{1}{D_{mi}} + \frac{1}{D_{ki}}}$	(6)	(Martins & Quinta-Ferreira, 2011)
The porosity of catalyst ( $\epsilon_B$ )	$\epsilon_B = V_g \rho_p$	(7)	(Xu <i>et al.</i> , 2018)
Particle density ( $\rho_p$ )	$\rho_p = \frac{\rho_B}{1 - \epsilon_B}$	(8)	(Xu <i>et al.</i> , 2018)
The tortuosity factor ( $\mathcal{T}$ )	The value of tortuosity factor ( $\mathcal{T}$ ) of the pore network ranged between (2 to 7)	---	(Aziz <i>et al.</i> , 2016)
The Knudsen diffusivity ( $D_{ki}$ )	$D_{ki} = 9700 r_g \left(\frac{T}{M_{w,ph}}\right)^{0.5}$	(9)	(Amor <i>et al.</i> , 2019)
Mean pore radius ( $r_g$ )	$r_g = \frac{2V_g}{S_g}$	(10)	(Amor <i>et al.</i> , 2019)
The molecular diffusivity ( $D_{mi}$ )	$D_{mi} = 8.93 * 10^{-8} \left(\frac{v_l^{0.267} T}{v_{ph}^{0.267} \mu_{ph}}\right)$	(11)	(Duduković, Larachi, & Mills, 2002; Paraskos, Frayer, & Shah, 1975)
The molar volume of the liquid ( $v_l$ )	$v_l = 0.285(v_{cl})^{1.048}$	(12)	(Lozano <i>et al.</i> , 2020)
The molar volume of the phenol compound ( $v_{ph}$ )	$v_{ph} = 0.285(v_{cph})^{1.048}$	(13)	(Lozano <i>et al.</i> , 2020)
The external volume of the catalyst (For sphere particle) ( $V_p$ )	$V_p = \frac{4}{3} \pi (r_p)^3$	(14)	(Amor <i>et al.</i> , 2019)
The external surface of the catalyst (For sphere particle) ( $S_p$ )	$S_p = 4\pi (r_p)^2$	(15)	(Amor <i>et al.</i> , 2019)
The phenol viscosity ( $\mu_{ph}$ )	$\mu_{ph} = \exp \left[ \ln(\alpha * \mu_{ph,b}) * \frac{\ln(\mu_{ph,b})}{\ln(\alpha * \mu_{ph,b})} \right]^\phi$	(16)	(Busca <i>et al.</i> , 2008)
Constant ( $\alpha$ )	0.1175 for alcohols and 0.248 for other compounds	---	(Amor <i>et al.</i> , 2019)
Volume fraction of molecule ( $\phi$ )	$\phi = \frac{1 - (T/T_c)}{1 - (T_b/T_c)}$	(17)	(Busca <i>et al.</i> , 2008)

$$X_{phenol} = 1 - \frac{C_{phenol}}{C_{phenol,t}} \tag{19}$$

### 4.3 Optimization problem formulation for evaluation of kinetic parameter

In this study, the expectation of the appropriate values of kinetic parameters is conducted by utilizing two approaches. These approaches are summarized below:

1. Linear regression: The kinetic parameters of reaction (constant of reaction rate ( $k$ ) and order of reaction ( $n$ )) are appreciated. Then, the Arrhenius equation is linearized so as to estimate the activation energy ( $EA$ ) and pre-exponential factor ( $k_0$ ).
2. Non-linear regression: In this approach, the evaluation of the kinetic parameters (the interaction order ( $n$ ), the pre-exponential factor ( $k_0$ ) and activation energy ( $EA$ )) is directly determined without a linearization step.

For estimating the optimal kinetic parameters for wet oxidation process, the optimization problem formulation configured as follows:

*Given:* The conditions oxidation reaction, the catalyst, and the reactor formation

*Determine:* Kinetic parameters ( $n$ ,  $k_0$  and  $EA$ ) for each designed catalyst.

*So, to reduce:* The sum of squared error (SSE).

*Subject to:* By calculating the mathematical operation constraints of the first method (the upper and lower constraints for the linear approach), the optimization problem is as follows:

**Table 3**  
Values of constant parameters applied in the modeling operation

Parameter, unit	Value
Initial concentration of phenol (Ct), ppm	634
reaction time min	20, 40, 60, 80,100,120
Reaction temperature (T1, T2, T3, T4), °C	303, 318, 333, 348
R, J/mole.°K	8.314
Vg (CAT-1, CAT-2, CAT-3), cm <sup>3</sup> /gm	0.139888, 0.120969, 0.134227
Sg (CAT-1, CAT-2, CAT-3), cm <sup>2</sup> /gm	535460, 486814, 371567
Vp (CAT-1, CAT-2, CAT-3), cm <sup>3</sup>	3.1759*10 <sup>-16</sup> , 3.9680*10 <sup>-16</sup> , 3.6061*10 <sup>-16</sup>
Sp (CAT-1, CAT-2, CAT-3), cm <sup>2</sup>	2.2511*10 <sup>-10</sup> , 2.9680*10 <sup>-10</sup> , 2.7474*10 <sup>-10</sup>
ρB. (CAT-1, CAT-2, CAT-3), gm/cm <sup>3</sup>	0.482, 0.534 ,0.556
M.Wt of phenol	184
r <sub>g</sub> , (CAT-1, CAT-2, CAT-3), nm	5.2249, 5.0757, 7.3701
v <sub>ct</sub> , cm <sup>3</sup> /gmole	55.95
v <sub>c,ph</sub> , cm <sup>3</sup> /gmole	229
T <sub>c</sub> , °R	1250

Min: SSE

$$n^j, EA^j, k_i^j, (i = 1 - 4, j = CAT_{1,2,3})$$

$$n^j = 1$$

S.t.  $f(z, x(z), \dot{x}(z), u(z), v) = 0$   
 $C_L \leq C \leq C_U$   
 $EA_L^j \leq EA^j \leq EA_U^j$   
 $k_{iL}^j \leq k_i^j \leq k_{iU}^j$

While by utilizing the 2<sup>nd</sup> method (nonlinear approach), the problem and the upper and lower constraints are presented as follow:

Min: SSE

$$n^j, EA^j, k_i^j, (i = 1 - 4, j = CAT_{1,2,3})$$

$$n^j \neq 1$$

S.t.  $f(z, x(z), \dot{x}(z), u(z), v) = 0$   
 $C_L \leq C \leq C_U$   
 $n_L^j \leq n^j \leq n_U^j$   
 $EA_L^j \leq EA^j \leq EA_U^j$   
 $k_{oL}^j \leq k_i^j \leq k_{oU}^j$

S.t.  $f(z, x(z), \dot{x}(z), u(z), v) = 0$ , describe the process model that presented previously.

- z : is the independent variable.
- u(z) : is the decision variable.
- x(z) : describe the set of variables.
- $\dot{x}(z)$  : describe the derivative of the variables with respect to time.
- v : is the design variable.
- C, C<sub>L</sub>, C<sub>U</sub> : concentration, lower and upper bounds of concentration, respectively.
- L, U : are the lower and upper bounds, respectively.

### 5. Maximizing of phenol elimination via optimizing operating conditions

The better value of kinetic parameters is utilized to determine the optimal operating conditions in which the maximum elimination of phenol is achieved. Therefore, the problem of optimization is created as follows:

*Obtain:* The optimal value of process conditions for high phenol elimination.

So, as to minimize: The concentration of phenol found in wastewater.

*Subjected to:* Constraints in the operation

The problem is mathematically expressed as follows:

Min  $C_{phenol}$   
 $T^j, time_i^j, C_{phenol}^j$  (j= CAT-1,2,3)

S.t.  $f(z, x(z), \dot{x}(z), u(z), v) = 0$   
 $time_L^j \leq time^j \leq time_U^j$   
 $C_{phenol.tL}^j \leq C_{phenol.t}^j \leq C_{phenol.tU}^j$   
 $T_L^j \leq T^j \leq T_U^j$   
 $X_{phenol.tL}^j \leq X_{phenol.t}^j \leq X_{phenol.tU}^j$

gPROMS software is utilized to conduct the optimization process.

### 6. Results and discussion

#### 6.1 Catalyst characterization

The surface area are 53.5460 m<sup>2</sup>/gm, 48.6814 m<sup>2</sup>/gm, 37.1567 m<sup>2</sup>/gm and the pore size are 10.44995 nm, 9.93963 nm, 14.44981 nm for Fe<sub>2</sub>O<sub>3</sub>, 2wt.% MnO<sub>2</sub>/Fe<sub>2</sub>O<sub>3</sub>, 5wt.% MnO<sub>2</sub>/Fe<sub>2</sub>O<sub>3</sub> catalysts, respectively. The results proved that the surface area for the prepared catalysts was decreased via enhancing the quantity of active metal oxide (MnO<sub>2</sub>) over catalyst support (Fe<sub>2</sub>O<sub>3</sub>). This behavior can be returned to the

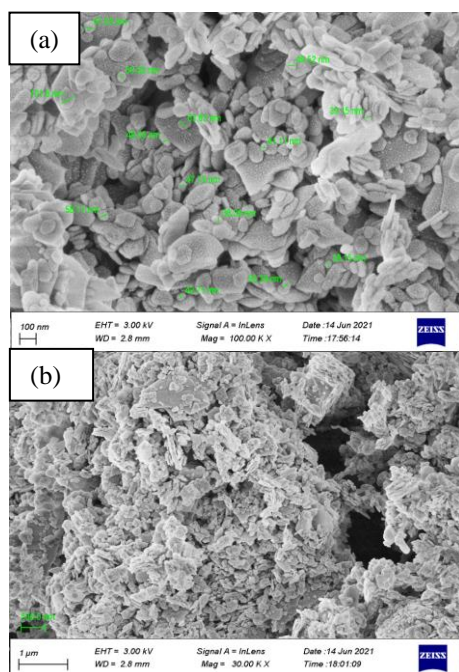


**Fig 2.** SEM of the prepared catalyst (2wt.%MnO<sub>2</sub>/Fe<sub>2</sub>O<sub>3</sub>) at a) 100 nm & b) 1 μm

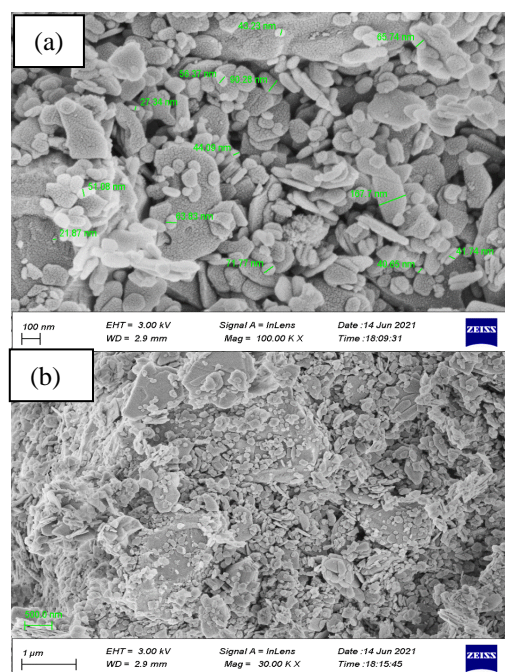


**Fig 3.** SEM of the prepared catalyst (5wt.%MnO<sub>2</sub>/Fe<sub>2</sub>O<sub>3</sub>) at a) 100 nm & b) 1 μm

significant occupation of the Fe<sub>2</sub>O<sub>3</sub> pores via MnO<sub>2</sub>. The deposition of active metal oxide in the pores of the catalyst support also led to blockage and interference in nitrogen diffusion (Aabid *et al.*, 2023; Fathi, Humadi, Mahmood, Nawaf, & Ayoub RS, 2022; Humadi *et al.*, 2022; Humadi *et al.*, 2023). The results of XRD patterns for the synthesis catalysts were explained in previous study (Hamad *et al.*, 2022a). The scanning electron microscope (SEM) for the synthesis (2% MnO<sub>2</sub>/Fe<sub>2</sub>O<sub>3</sub>) and (5% MnO<sub>2</sub>/Fe<sub>2</sub>O<sub>3</sub>) catalysts were showed in Figures 2 and 3. These results explained a uniform distribution of active metal oxide particles (MnO<sub>2</sub>) over catalyst support (Fe<sub>2</sub>O<sub>3</sub>). Also, the obtained images proved that the synthesis catalysts were nano sizes particles.

## 6.2 Catalytic phenol oxidation

### 6.2.1 Effect of MnO<sub>2</sub> loaded

Three catalysts were prepared by loading different concentrations of MnO<sub>2</sub> (0%, 2% and 5%) on Fe<sub>2</sub>O<sub>3</sub>. Figure 4 shows the effect of MnO<sub>2</sub> loading on the activity of phenol oxidation. The results showed that the oxidation activity of phenol increases linearly with the increase of MnO<sub>2</sub> loading. Also, the results showed stable activity for catalyst through all times without deactivation effects (Hamad *et al.*, 2022a; Humadi *et al.*, 2022). This behavior can be returned to that the dispersion of MnO<sub>2</sub> on the Fe<sub>2</sub>O<sub>3</sub> differs based on the active metal oxide loading, the activity of wet catalytic phenol oxidation process may change as a result (Hamad *et al.*, 2022a; Humadi *et al.*, 2023). In the consecutive experiments, the same catalyst was used without the replacing. There results proved the remarkability durability and lifetime for preparing catalyst. The results proved that 5wt.% MnO<sub>2</sub>/Fe<sub>2</sub>O<sub>3</sub> achieved phenol removing of 94wt.% during 80 min or reaction time. In comparing with other used catalyst under the same reaction time, 80wt.% or less for 2wt.% MnO<sub>2</sub>/Fe<sub>2</sub>O<sub>3</sub> and 71wt.% for only Fe<sub>2</sub>O<sub>3</sub>. These results can be attributed to that Mn coordination are stretched along z-axis of Mn atoms as a result of Jahn-Teller phenomenon (Li *et al.*, 2014), causing deforming octahedral or tetragonal structure. Thus, larger space phenol is supplied to

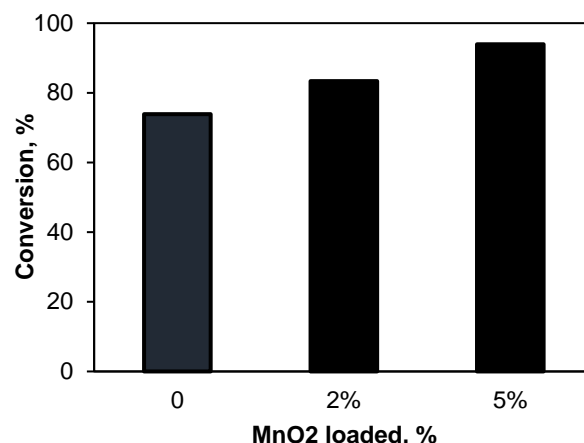


**Fig 4.** The effect of MnO<sub>2</sub> loaded on the phenol oxidation activity

approach the core Mn ion. Also, Mn atoms have high redox potential.

### 6.2.2 Influence of reaction time

Figure 5 shows the impact of oxidation time on phenol elimination using the best catalyst 5 % MnO<sub>2</sub>/Fe<sub>2</sub>O<sub>3</sub>. The removal of phenol under 30°C was very low for the whole evaluated oxidation time. Under the maximum temperatures of 60°C and 70°C, the phenol removal shows high and significantly under the lower oxidation time of 20 min. The reason of such behavior can be return to a fast adsorption (physically) on the surface of MnO<sub>2</sub>/Fe<sub>2</sub>O<sub>3</sub> which led to the initial phenol removal. Increasing of time progressively improved the phenol oxidation up to 80 min (Aabid *et al.*, 2023; Humadi, Ghenni, Ahmed, & Harvey, 2022; Humadi *et al.*, 2022). The results proved that the performance wet oxidation process improves by rising reaction times, as enhancing contacting time between the reactants (Adamu, Dubey, & Anderson, 2016; Hamad *et al.*,

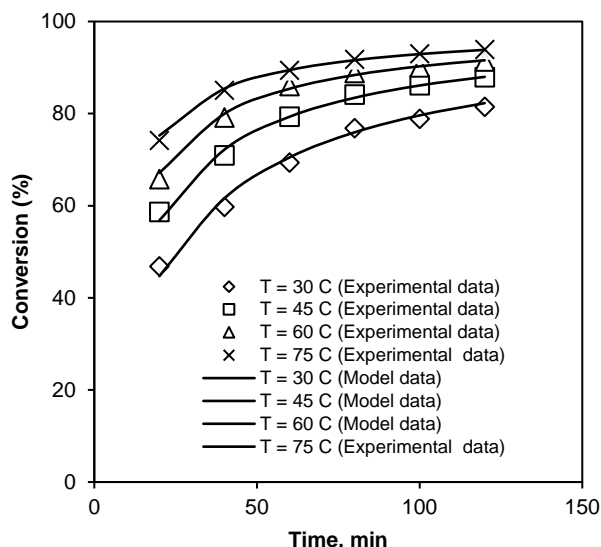


Fig 5. The effect of reaction time on the phenol oxidation activity for CAT-3

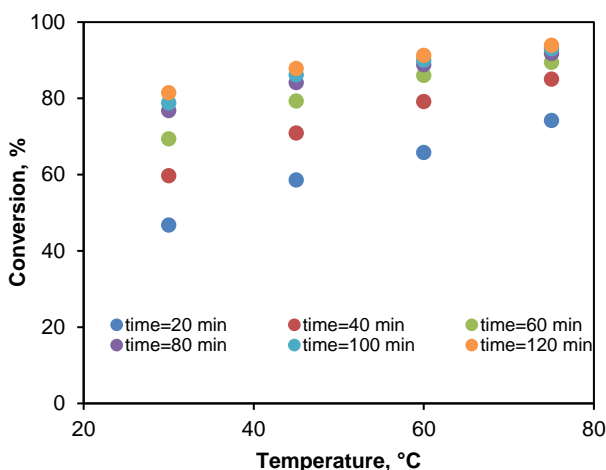


Fig 6. The effect of reaction temperature on the phenol oxidation activity for CAT-3

2022a; Jafar, Nawaf, & Humadi, 2021; Luo *et al.*, 2015), H<sub>2</sub>O<sub>2</sub> improve the transfer of oxygen atoms and phenol in the MnO<sub>2</sub>/Fe<sub>2</sub>O<sub>3</sub> pores. More enhancing in time is proved the stable results in removing of phenol up to 120 min. These obtained data can be returned to consume large amount of H<sub>2</sub>O<sub>2</sub> through the oxidation process. The experimental data showed that 5wt.% MnO<sub>2</sub>/Fe<sub>2</sub>O<sub>3</sub> achieved phenol removing of 94wt.% during 80 min or reaction time. At the same oxidation time, 80wt.% or less for 2wt.% MnO<sub>2</sub>/Fe<sub>2</sub>O<sub>3</sub> and 71wt.% for only Fe<sub>2</sub>O<sub>3</sub> was achieved. Under various times for CWPO, there are nil content of reaction intermediates.

6.2.3 Influence of reaction temperature

The temperature in CWPO is important process variable. The impact of various temperatures on the performance of CWPO was investigated. As shown in Figure 6, the catalytic oxidation of phenol was promoted by increasing the reaction temperature of all designed catalysts. This is because the increase of the reaction temperature will lead to the dissociation of H<sub>2</sub>O<sub>2</sub> in the wastewater leading to an increase in the generation of hydroxyl radicals (Fathi *et al.*, 2022; Humadi *et al.*, 2021; Jafar *et al.*, 2021; Zazo, Pliego, Blasco, Casas, & Rodriguez, 2011). Furthermore, increasing the reaction temperature may lead to a significant

increase in H<sub>2</sub>O<sub>2</sub> consumption and decomposition of organic pollutants in wastewater (Rueda Márquez, Levchuk, & Sillanpää, 2018). Increasing of the performance of wet oxidation process via enhancing the reaction temperature can be attributed also to improve the activation energy which led to improve the diffusion phenol and oxygen molecules inside the pores of MnO<sub>2</sub>/Fe<sub>2</sub>O<sub>3</sub>. Therefore, this behavior of oxidation process improved via increasing temperature due to the higher impact of temperature factor on phenol removal from waste water (Humadi *et al.*, 2021; Humadi *et al.*, 2022; Inchaurredo, Massa, Fenoglio, Font, & Haure, 2012). Gao *et al.* (2018) examined the impact of different temperatures (70°C, 80°C, and 90°C) on CWPO performance using Fe<sub>2</sub>O<sub>3</sub>-CeO<sub>2</sub>-Bi<sub>2</sub>O<sub>3</sub>/γ-Al<sub>2</sub>O<sub>3</sub> as catalyst. They explained that increasing of temperature improved the phenol removing efficiency from 18 to 76wt.% after the 240 min reaction. This study used simpler catalyst which showed significant activity in eliminating of phenol under mild conditions.

6.3 Evaluating results of kinetic parameters

6.3.1 Results of linear regression

For each prepared catalyst, the optimal value of model parameters specified by applying the linear methods is summarized in the following Tables 4 - 6. As shown in these Tables, the order of catalytic phenol oxidation reactions was reported to be 3.46 for CAT-1, 2.7 for CAT-2 and 1.98 for CAT-3 for phenolic compounds found in wastewater. Kinetic parameters (activation energy (E<sub>A</sub>) and Frequency factor (k<sub>0</sub>)) are determined by plotting of (lnk) versus (1/T) as shown in Figure 7 for each prepared catalyst.

The kinetic parameters values (E<sub>A</sub> and k<sub>0</sub>) obtained are illustrated in Table 7. As shown in Table 7, the catalyst type significantly affects the activation energy. In this work, the activation energies of phenolic compounds in wastewater are 28.714 kJ/mol for CAT-1, 26 kJ/mol for CAT-2 and 26.4 kJ/mol for CAT-3.

6.3.2 Results of non-linear regression

Kinetic parameters (n, E<sub>A</sub> and k<sub>0</sub>) for the catalytic phenol oxidation have been evaluated based on nonlinear methods, and the values of these parameters are described in Tables S1 – S3. According to the results summarized in these Tables, CAT-3

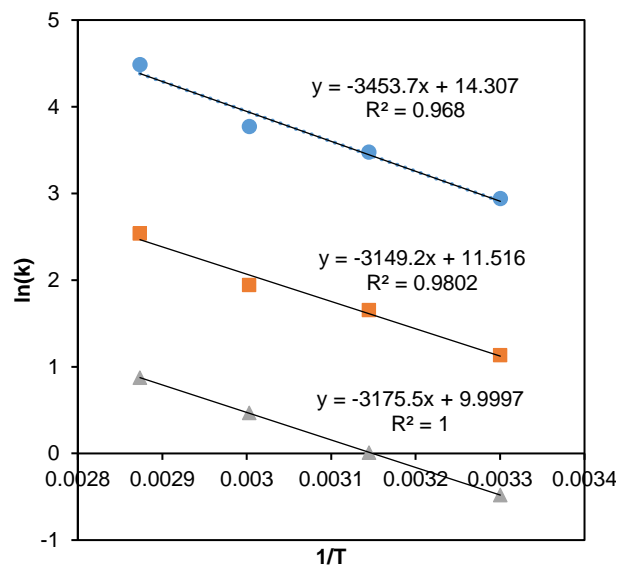


Fig 7. lnk versus (1/T) for kinetic parameters of the catalytic oxidation process using different prepared catalysts.

**Table 4**  
Optimal values of model parameters are optimized using the linear method of CAT-1

Parameter	Value	Unit
n	3.463377	–
k1	18.90354	$(wt^{-2.463377}).min^{-1}$
k2	32.36415	$(wt^{-2.463377}).min^{-1}$
k3	43.39928	$(wt^{-2.463377}).min^{-1}$
k4	88.81517	$(wt^{-2.463377}).min^{-1}$
SSE	$2.8000 \times 10^{-5}$	–

**Table 5**  
Optimal values of model parameters are optimized using the linear method of CAT-2

Parameter	Value	Unit
n	2.707247	–
k1	3.107599	$(wt^{-1.707247}).min^{-1}$
k2	5.213272	$(wt^{-1.707247}).min^{-1}$
k3	6.962609	$(wt^{-1.707247}).min^{-1}$
k4	12.61321	$(wt^{-1.707247}).min^{-1}$
SSE	$1.6537 \times 10^{-5}$	–

**Table 6**  
Optimal values of model parameters are optimized using the linear method of CAT-3

Parameter	Value	Unit
n	1.982137	–
k1	0.6192847	$(wt^{-0.982137}).min^{-1}$
k2	1.0099570	$(wt^{-0.982137}).min^{-1}$
k3	1.5946560	$(wt^{-0.982137}).min^{-1}$
k4	2.3959250	$(wt^{-0.982137}).min^{-1}$
SSE	$9.2137 \times 10^{-6}$	–

clearly outperforms the other catalysts based on the values of reaction order and activation energy under the same process conditions. The reaction order and activation energy values of CAT-3 are lower than the other catalysts, which mean that the reaction in the presence of CAT-3 occurs faster than the other catalysts.

6.3.2 Comparison between linear and nonlinear approaches

Figure 8 are explained the comparison between experimental and simulated data for different prepared catalyst based on the linear and nonlinear regressions. Based on these results for all types of used catalyst, the error between the experimental and predicted results based on the nonlinear approach is less than the error obtained by the linear approach for all runs. This behaviour can be returned to that the nonlinear approach predict the actual kinetic parameters which used in evaluating the conversion in comparing with the linear approach that assumed

the order or reaction equal to 1 and evaluated the conversion based on that with more error.

Table 8 showed the comparison between the kinetic parameters for the linear and nonlinear regressions. Based on the obtained results, the activation energy for the linear model is lower than that for the nonlinear model using CAT1 and CAT2

**Table 7**  
Kinetic parameter values (EA and ko) for each prepared catalyst

Catalyst	EA (kJ/mol)	Frequency factor
CAT-1	28.714	1634749.271
CAT-2	26.182	100307.926
CAT-3	26.401	22019.858

**Table 8**  
Comparison between the kinetic parameters for the linear and nonlinear regressions

Parameter	Linear	Non linear
<b>CAT1</b>		
Reaction order, n	3.463377	3.36
Frequency factor, Ko	$1.6348 \times 10^6$	$2.0596 \times 10^6$
Activation energy, $E_A$ (kJ/mol)	28.714	30.080
<b>CAT2</b>		
Reaction order, n	2.707247	2.75
Frequency factor, Ko	$1.0031 \times 10^5$	$2.0711 \times 10^5$
Activation energy, $E_A$ (kJ/mol)	26.182	27.599
<b>CAT3</b>		
Reaction order, n	1.982137	1.98
Frequency factor, Ko	22020	20952
Activation energy, $E_A$ (kJ/mol)	26.401	26.254

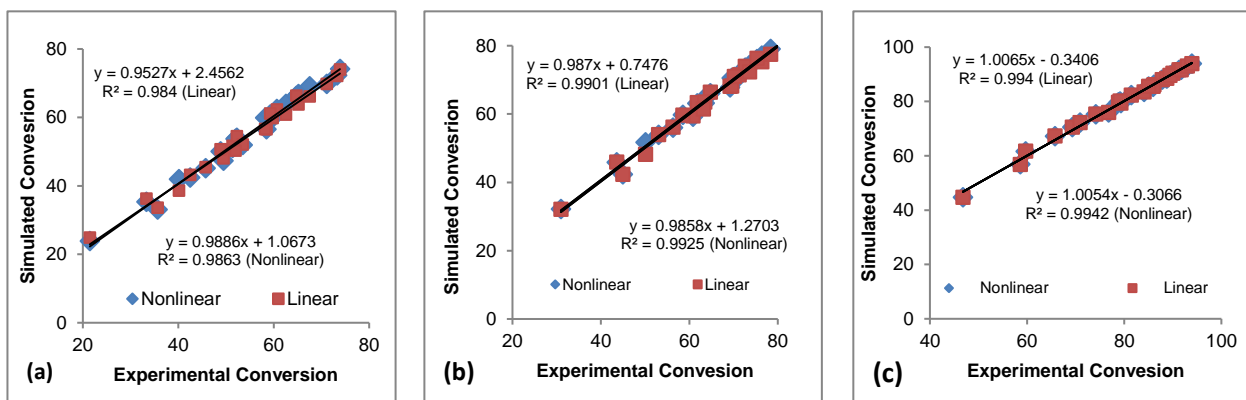


**Fig 8.** Comparison between experimental and simulated data for different prepared catalyst based on the linear and nonlinear regressions, (a) for CAT 1, (b) for CAT 2, and (c) for cat 3.

but it is approximately similar for the tow regressions using CAT3. The low activation energy for all prepared catalyst proved that the wet catalytic phenol oxidation process is more efficient and the phenol oxidation reaction is faster (Ahmad & Ahmad, 2017; Humadi *et al.*, 2022; Ibrahim, Noori, & Khasbag, 2016). The phenol oxidation reactivity enhances via increasing the electron density of the phenol and this cause the decreasing in the activation energy (Humadi, Ghenni, et al., 2022; Sachdeva & Pant, 2010). The low activation energy results can be returned to the electrophilic addition of oxygen or the high electron density on phenol.

These results for the activation energy might be driving forces compel phenol which is thermally lower staggered in reacting with the  $H_2O_2$ , and improve the performance of oxidation process (Borah, 2006; Hasan, Jeon, & Jung, 2012; Humadi *et al.*, 2022). The results showed that the frequency factor for the nonlinear model is lower than that for the linear model using CAT1 and CAT2 but it is higher using CAT3. In general, the low pre-exponential factor of wet catalytic phenol oxidation process referred to the no spontaneity of phenol

oxidation reaction (Borah, 2006; Humadi, Ghenni, et al., 2022). Since the sum of squared errors (SSE) of the nonlinear regression is lower than that of the linear regression, so more accurate optimal parameters are obtained by applying the nonlinear regression.

#### 6.4 Experimental and simulation results

The simulation process was carried out by using gPROMS software. The experimental results and prediction results are shown in Tables S4 to S9. As can be seen from these Tables, the optimal kinetic parameters predicted by the modeling process gave accurate results with low error (<5%) for all prepared catalysts. Furthermore, since the sum of squared errors (SSE) of the nonlinear method is lower than that of the linear method described in Table 9, more accurate optimal parameters are obtained by applying the nonlinear method.

Additionally, Figures 9 shows a parity plot between the experimental run results and the results predicted by the modeling process. As shown, the correlation between the

**Table 9**  
Comparison between sum of squared errors (SSE)

Parameters	Sum of squared errors (SSE)	
	Linear approach	Non-linear approach
CAT-1	$28.00 \times 10^{-6}$	$24.500 \times 10^{-6}$
CAT-2	$16.537 \times 10^{-6}$	$13.750 \times 10^{-6}$
CAT-3	$87.057 \times 10^{-7}$	$92.137 \times 10^{-7}$

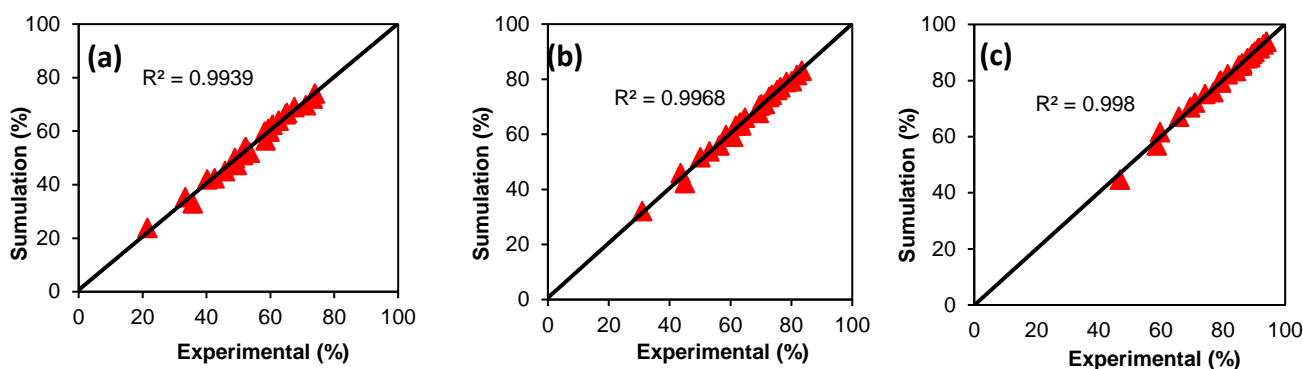


**Fig 9.** Comparison between experimental and simulated data for different prepared catalyst, (a) for CAT 1, (b) for CAT 2, and (c) for CAT 3.

experimental and predicted data appears to be a straight line with a slope close to 1.0, indicating a high match between the experimental and predicted results.

At various conditions (catalyst types, temperatures, and times), the obtained data experimentally and by modeling technique showed much acceptable error (<5%) as shown in Figures 9. According to these data, the experimental and predicted runs are remarkably agreed at the same CWPO conditions.

*6.5 Results of optimal process conditions for maximum removal of phenol*

The optimal process conditions specified by applying the optimization process to each prepared catalyst are summarized in Table 10 below. According to the results explained in this Table, the maximum performance for CWPO was 84.5%, 90.1%, and 98% which achieved via 5wt.% MnO<sub>2</sub>/Fe<sub>2</sub>O<sub>3</sub> at (779 ppm, 67 °C, 295 min), 2wt.% MnO<sub>2</sub>/Fe<sub>2</sub>O<sub>3</sub> (791 ppm, 61 °C, 280 min), and Fe<sub>2</sub>O<sub>3</sub> (764 ppm, 70 °C, 294 min), respectively to meet the environmental regulations for keeping fresh water without harmful impurities. These results proved that the maximum phenol removal efficiency was obtained via enhancing oxidation temperature and oxidation time. Also, the results of phenol

oxidation process was improved and maximized via selecting efficient process model under optimal conditions. The obtained data proved that the maximum phenol removal was achieved under mild operating conditions. The maximum phenol removing efficiency was (98%) under the obtained optimal conditions. So that, eco-friendly fresh water was regarded the important objective this study.

**7 Conclusions**

In this study, a novel nano-catalyst (MnO<sub>2</sub>/Fe<sub>2</sub>O<sub>3</sub>) was prepared to catalyze the phenol oxidation process. The effect of operating conditions on the oxidation process was experimentally investigated in the presence of the prepared catalysts. It has been concluded that 70°C is the final temperature for phenol oxidation as oxidation; above this temperature tends to decompose the hydrogen peroxide and lose the strength of the oxidant. The three nano-catalyst were also found to resist deactivation and show stable performance by enduring operation for a long time. Simulation and optimization techniques were used to determine the optimal kinetic values of the prepared phenol oxidation catalysts nonlinear regression

**Table 10**  
Optimal process conditions for phenol oxidation using the prepared catalysts

Parameter, unit	Values		
	CAT-1	CAT-2	CAT-3
C <sub>phenol,t</sub> , ppm	779	791	764
T, °C	67	61	70
Time, min	295	280	294
Conversion, %	84.5	90.1	98

was found to be more accurate for calculation the sum of square errors (SEE). Based on the optimal kinetic parameters, the highest conversion of CAT-3 phenol was 98% at 70°C, a residence time of 294 min, and an initial phenol concentration of 764 ppm.

## Nomenclature

$C_{ph}$	Phenol Concentration (mol/cm <sup>3</sup> )
$X_{ph}$	Conversion of phenol (-)
$C_{ph}$	Concentration of phenol at the end of the reaction (mol/cm <sup>3</sup> )
$C_{ph,t}$	Initial concentration of phenol present in wastewater (mol/cm <sup>3</sup> )
$k$	Reaction Rate Constant
$k_{App}$	Apparent Rate Constant
$D_{ei}$	Effective diffusivity (cm <sup>2</sup> /s)
$D_{ki}$	Knudsen diffusivity
$D_{mi}$	Molecular diffusivity (cm <sup>2</sup> /s)
$EA$	Activation Energy (J/mol K)
$M_{w,ph}$	Molecular weight of phenol (gm/gmol)
$T_c$	Critical temperature of phenol (°R)
$T_b$	Boiling point temperature of phenol (°C)
$T_{br}$	Reduced boiling point temperature
$T_r$	Reduced temperature
$R$	Gas constant (J/mol K)
$n$	Order of reaction
$-T_{ph}$	Reaction rate of phenol
$r_g$	Pore radius (nm)
$r_p$	Particle radius (nm)
$S_p$	External surface area of catalyst particle (cm <sup>2</sup> /gm)
$S_g$	Specific surface area of particle (cm <sup>2</sup> )
$V_p$	External Volume of catalyst particle (cm <sup>3</sup> )
$V_g$	Pore volume (cm <sup>3</sup> /gm)
$v_l$	Liquid molar volume
$v_{cl}$	Critical molar volume of liquid (cm <sup>3</sup> /gmole)
$v_{ph}$	Molar volume of phenol
$v_{c,ph}$	Critical volume of phenol (cm <sup>3</sup> /gmole)

## Greek Symbols

$\eta_0$	Effectiveness factor
$\alpha$	Constant factor
$\Phi$	Volume fraction of molecule
$\epsilon_B$	Porosity
$\mathcal{T}$	Tortuosity
$\rho_B$	Bulk density (gm/cm <sup>3</sup> )
$\rho_p$	Particle density (gm/cm <sup>3</sup> )
$\mu_{ph}$	Viscosity of phenol (mPa s)
$\mu_{ph,b}$	Viscosity of phenol at boiling point (mPa s)
$0$	Initial (at time = 0)

## Supplementary Information

Supplementary information is available at <https://ejournal.undip.ac.id/index.php/ijred/article/download/SuppFile/52044/13297>

Supplementary material associated with this manuscript contains the following:

Optimal values of kinetic parameters are optimized using the nonlinear method of CAT-1, optimal values of kinetic parameters are optimized using the nonlinear method of CAT-2, optimal values of kinetic parameters are optimized using the nonlinear method of CAT-3, experimental and simulation results using the nonlinear method of CAT-1, experimental and simulation results using the nonlinear method of CAT-2, experimental and simulation results using the nonlinear method of CAT-3, experimental and simulation results using the linear method of CAT-1, experimental and simulation results using the linear method of CAT-2, and experimental and simulation results using the linear method of CAT-3.

## Conflicts of Interest

The authors declare no conflict of interests.

## Acknowledgments

This research did not receive any specific grant from funding agencies in the public, commercial, or non-for-profit sectors.

## References

- Aabid, A. A., Humadi, J. I., Ahmed, G. S., Jarullah, A. T., Ahmed, M. A., & Abdullah, W. S. (2023). Enhancement of Desulfurization Process for Light Gas Oil Using New Zinc Oxide Loaded Over Alumina Nanocatalyst. <https://doi.org/10.14416/j.asep.2023.02.007>
- Adamu, H., Dubey, P., & Anderson, J. A. (2016). Probing the role of thermally reduced graphene oxide in enhancing performance of TiO<sub>2</sub> in photocatalytic phenol removal from aqueous environments. *Chemical engineering journal*, 284, 380-388. <https://doi.org/10.1016/j.cej.2015.08.147>
- Ahmad, W., & Ahmad, I. (2017). Desulfurization of transportation fuels by per-formic acid oxidant using MoO<sub>x</sub> loaded on ZSM-5 catalyst. *Journal of Power and Energy Engineering*, 5(12), 87-99. <https://doi.org/10.4236/jpee.2017.512011>
- Ahmed, M., El-Katori, E. E., & Gharni, Z. H. (2013). Photocatalytic degradation of methylene blue dye using Fe<sub>2</sub>O<sub>3</sub>/TiO<sub>2</sub> nanoparticles prepared by sol-gel method. *Journal of Alloys and Compounds*, 553, 19-29. <https://doi.org/10.1016/j.jallcom.2012.10.038>
- Amor, C., Rodriguez-Chueca, J., Fernandes, J. L., Dominguez, J. R., Lucas, M. S., & Peres, J. A. (2019). Winery wastewater treatment by sulphate radical based-advanced oxidation processes (SR-AOP): Thermally vs UV-assisted persulphate activation. *Process Safety and Environmental Protection*, 122, 94-101. <https://doi.org/10.1016/j.psep.2018.11.016>
- Amor, L., Eiroa, M., Kennes, C., & Veiga, M. C. (2005). Phenol biodegradation and its effect on the nitrification process. *Water research*, 39(13), 2915-2920. <https://doi.org/10.1016/j.watres.2005.05.019>
- Aziz, A. R. A., Asaithambi, P., & Daud, W. M. A. B. W. (2016). Combination of electrocoagulation with advanced oxidation processes for the treatment of distillery industrial effluent. *Process Safety and Environmental Protection*, 99, 227-235. <https://doi.org/10.1016/j.psep.2015.11.010>
- Baloyi, J., Ntho, T., & Moma, J. (2018). Synthesis and application of pillared clay heterogeneous catalysts for wastewater treatment: a review. *RSC Advances*, 8(10), 5197-5211. <https://doi.org/10.1039/C7RA12924F>
- Borah, D. (2006). Desulfurization of organic sulfur from a subbituminous coal by electron-transfer process with K<sub>4</sub>[Fe(CN)<sub>6</sub>]. *Energy & Fuels*, 20(1), 287-294. <https://doi.org/10.1021/ef050340b>
- Busca, G., Berardinelli, S., Resini, C., & Arrighi, L. (2008). Technologies for the removal of phenol from fluid streams: a short review of recent developments. *Journal of hazardous materials*, 160(2-3), 265-288. <https://doi.org/10.1016/j.jhazmat.2008.03.045>
- Covinich, L. G., Bengoechea, D. I., Fenoglio, R. J., & Area, M. C. (2014). Advanced oxidation processes for wastewater treatment in the pulp and paper industry: a review. *American Journal of Environmental Engineering*, 4(3), 56-70. <https://doi.org/10.5923/j.ajee.20140403.03>
- Duduković, M. P., Larachi, F., & Mills, P. L. (2002). Multiphase catalytic reactors: a perspective on current knowledge and future trends. *Catalysis Reviews*, 44(1), 123-246. <https://doi.org/10.1081/CR-120001460>
- Esplugas, S., Gimenez, J., Contreras, S., Pascual, E., & Rodríguez, M. (2002). Comparison of different advanced oxidation processes for phenol degradation. *Water research*, 36(4), 1034-1042. [https://doi.org/10.1016/S0043-1354\(01\)00301-3](https://doi.org/10.1016/S0043-1354(01)00301-3)
- Fathi, M. I., Humadi, J. I., Mahmood, Q. A., Nawaf, A. T., & Ayoub RS, R. S. (2022). Improvement of design synthetic nano-catalysts for performance enhancement of oxidative desulfurization using batch reactor. Paper presented at the AIP Conference Proceedings. <https://doi.org/10.1063/5.0109089>
- Fei, J., Sun, L., Zhou, C., Ling, H., Yan, F., Zhong, X., Liu, Z. (2017). Tuning the synthesis of manganese oxides nanoparticles for efficient oxidation of benzyl alcohol. *Nanoscale research letters*, 12(1), 1-9. <https://doi.org/10.1186/s11671-016-1777-y>
- Gagol, M., Cako, E., Fedorov, K., Soltani, R. D. C., Przyjazny, A., & Boczkaj, G. (2020). Hydrodynamic cavitation based advanced oxidation processes: Studies on specific effects of inorganic acids on the degradation effectiveness of organic pollutants. *Journal of Molecular Liquids*, 307, 113002. <https://doi.org/10.1016/j.molliq.2020.113002>

- Gao, P., Song, Y., Wang, S., Descorme, C., & Yang, S. (2018). Fe<sub>2</sub>O<sub>3</sub>-CeO<sub>2</sub>-Bi<sub>2</sub>O<sub>3</sub>/γ-Al<sub>2</sub>O<sub>3</sub> catalyst in the catalytic wet air oxidation (CWAO) of cationic red GTL under mild reaction conditions. *Frontiers of Environmental Science & Engineering*, 12(1), 1-8. <https://doi.org/10.1007/s11783-018-1025-z>
- Hamad, K. I., Humadi, J. I., Issa, Y. S., Ghenni, S. A., Ahmed, M. A., & Hassan, A. A. (2022a). Enhancement of activity and lifetime of nano-iron oxide catalyst for environmentally friendly catalytic phenol oxidation process. *Cleaner Engineering and Technology*, 11, 100570. <https://doi.org/10.1016/j.clet.2022.100570>
- Hamad, K. I., Humadi, J. I., Issa, Y. S., Ghenni, S. A., Ahmed, M. A., & Hassan, A. A. (2022b). Enhancement of activity and lifetime of nano-iron oxide catalyst for environmentally friendly catalytic phenol oxidation process. *Cleaner Engineering and Technology*, 100570. <https://doi.org/10.1016/j.clet.2022.100570>
- Hasan, Z., Jeon, J., & Jung, S. H. (2012). Oxidative desulfurization of benzothiophene and thiophene with WO<sub>x</sub>/ZrO<sub>2</sub> catalysts: effect of calcination temperature of catalysts. *Journal of hazardous materials*, 205, 216-221. <https://doi.org/10.1016/j.jhazmat.2011.12.059>
- Hu, E., Pan, S., Zhang, W., Zhao, X., Liao, B., & He, F. (2019). Impact of dissolved O<sub>2</sub> on phenol oxidation by δ-MnO<sub>2</sub>. *Environmental Science: Processes & Impacts*, 21(12), 2118-2127. <https://doi.org/10.1039/C9EM00389D>
- Huang, P., Luo, G., Kang, L., Zhu, M., & Dai, B. (2017). Preparation, characterization and catalytic performance of HPW/aEVM catalyst on oxidative desulfurization. *RSC Advances*, 7(8), 4681-4687. <https://doi.org/10.1039/C6RA26587A>
- Humadi, J. I., Ghenni, S. A., Ahmed, S. M., Abdullah, G. H., Phan, A. N., & Harvey, A. P. (2021). Fast, non-extractive, and ultradeep desulfurization of diesel in an oscillatory baffled reactor. *Process Safety and Environmental Protection*, 152, 178-187. <https://doi.org/10.1016/j.psep.2021.05.028>
- Humadi, J. I., Ghenni, S. A., Ahmed, S. M., & Harvey, A. (2022). Dimensionless evaluation and kinetics of rapid and ultradeep desulfurization of diesel fuel in an oscillatory baffled reactor. *RSC Advances*, 12(23), 14385-14396. <https://doi.org/10.1039/D2RA01663J>
- Humadi, J. I., Issa, Y. S., Aqar, D. Y., Ahmed, M. A., Ali Alak, H. H., & Mujtaba, I. M. (2022). Evaluation of the performance of the tin (IV) oxide (SnO<sub>2</sub>) in the removal of sulfur compounds via oxidative-extractive desulfurization process for production an eco-friendly fuel. *International Journal of Chemical Reactor Engineering*(0). <https://doi.org/10.1515/ijcre-2022-0046>
- Humadi, J. I., Nawaf, A. T., Jarullah, A. T., Ahmed, M. A., Hameed, S. A., & Mujtaba, I. M. (2023). Design of new nano-catalysts and digital basket reactor for oxidative desulfurization of fuel: Experiments and modelling. *Chemical Engineering Research and Design*, 190, 634-650. <https://doi.org/10.1016/j.cherd.2022.12.043>
- Humadi, J. I., Nawaf, A. T., Khamees, L. A., Abd-Allahussain, Y. A., Muhsin, H. F., Ahmed, M. A., & Ahmed, M. M. (2022). Development of new effective activated carbon supported alkaline adsorbent used for removal phenolic compounds from refinery waste water in a fixed bed adsorption column. <https://doi.org/10.21203/rs.3.rs-2210259/v1>
- Ibrahim, N. K., Noori, W. A., & Khasbag, J. M. (2016). Ultrasound-Assisted Oxidative Desulfurization of Diesel. *Journal of Engineering*, 22(11), 55-67. <https://joe.uobaghdad.edu.iq/index.php/main/article/view/121>
- Inchaurrondo, N., Massa, P., Fenoglio, R., Font, J., & Haure, P. (2012). Efficient catalytic wet peroxide oxidation of phenol at moderate temperature using a high-load supported copper catalyst. *Chemical engineering journal*, 198, 426-434. <https://doi.org/10.1016/j.cej.2012.05.103>
- Iniesta, J., González-García, J., Exposito, E., Montiel, V., & Aldaz, A. (2001). Influence of chloride ion on electrochemical degradation of phenol in alkaline medium using bismuth doped and pure PbO<sub>2</sub> anodes. *Water research*, 35(14), 3291-3300. [https://doi.org/10.1016/S0043-1354\(01\)00043-4](https://doi.org/10.1016/S0043-1354(01)00043-4)
- Jafar, S. A., Nawaf, A. T., & Humadi, J. I. (2021). Improving the extraction of sulfur-containing compounds from fuel using surfactant material in a digital baffle reactor. *Materials Today: Proceedings*, 42, 1777-1783. <https://doi.org/10.1016/j.matpr.2020.11.821>
- Khasawneh, O. F. S., & Palaniandy, P. (2021). Removal of organic pollutants from water by Fe<sub>2</sub>O<sub>3</sub>/TiO<sub>2</sub> based photocatalytic degradation: A review. *Environmental Technology & Innovation*, 21, 101230. <https://doi.org/10.1016/j.eti.2020.101230>
- Kumar, A., Kumar, S., & Kumar, S. (2005). Biodegradation kinetics of phenol and catechol using *Pseudomonas putida* MTCC 1194. *Biochemical Engineering Journal*, 22(2), 151-159. <https://doi.org/10.1016/j.bej.2004.09.006>
- Li, A., Zhang, Q., Zhang, G., Chen, J., Fei, Z., & Liu, F. (2002). Adsorption of phenolic compounds from aqueous solutions by a water-compatible hypercrosslinked polymeric adsorbent. *Chemosphere*, 47(9), 981-989. [https://doi.org/10.1016/S0045-6535\(01\)00222-3](https://doi.org/10.1016/S0045-6535(01)00222-3)
- Li, X.-y., Cui, Y.-h., Feng, Y.-j., Xie, Z.-m., & Gu, J.-D. (2005). Reaction pathways and mechanisms of the electrochemical degradation of phenol on different electrodes. *Water research*, 39(10), 1972-1981. <https://doi.org/10.1016/j.watres.2005.02.021>
- Li, X., Ma, X., Su, D., Liu, L., Chisnell, R., Ong, S. P., . . . Lei, Y. (2014). Direct visualization of the Jahn-Teller effect coupled to Na ordering in Na<sub>5</sub>/8MnO<sub>2</sub>. *Nature materials*, 13(6), 586-592. <https://doi.org/10.1038/nmat3964>
- Lokhat, D., Oliver, M., & Carsky, M. (2015). Preparation of iron oxide nanocatalysts and application in the liquid phase oxidation of benzene. *Polish Journal of Chemical Technology*, 17(2). <https://doi.org/10.1515/pjct-2015-0027>
- Lozano, L. A., Devard, A., Ulla, M. A., & Zamaro, J. M. (2020). Cu/U<sub>2</sub>O<sub>6</sub>: A novel nanocatalyst obtained by a microwave-assisted protocol in DMF-free media for the efficient phenol removal via catalytic wet peroxide oxidation. *Journal of Environmental Chemical Engineering*, 8(5), 104332. <https://doi.org/10.1016/j.jece.2020.104332>
- Luo, H., Li, C., Wu, C., Zheng, W., & Dong, X. (2015). Electrochemical degradation of phenol by in situ electro-generated and electro-activated hydrogen peroxide using an improved gas diffusion cathode. *Electrochimica Acta*, 186, 486-493. <https://doi.org/10.1016/j.electacta.2015.10.194>
- Luo, L., Dai, C., Zhang, A., Wang, J., Liu, M., Song, C., & Guo, X. (2015). A facile strategy for enhancing FeCu bimetallic promotion for catalytic phenol oxidation. *Catalysis Science & Technology*, 5(6), 3159-3165. <https://doi.org/10.1039/C5CY00242G>
- Martin-Martinez, M., Barreiro, M., Silva, A., Figueiredo, J., Faria, J., & Gomes, H. (2016). Lignin-derived carbon materials as catalysts for wet peroxide oxidation. *Carbon* 2016. <https://hdl.handle.net/10198/17105>
- Martins, R. C., & Quinta-Ferreira, R. M. (2011). Remediation of phenolic wastewaters by advanced oxidation processes (AOPs) at ambient conditions: Comparative studies. *Chemical Engineering Science*, 66(14), 3243-3250. <https://doi.org/10.1016/j.ces.2011.02.023>
- Pan, B., Xiong, Y., Su, Q., Li, A., Chen, J., & Zhang, Q. (2003). Role of amination of a polymeric adsorbent on phenol adsorption from aqueous solution. *Chemosphere*, 51(9), 953-962. [https://doi.org/10.1016/S0045-6535\(03\)00038-9](https://doi.org/10.1016/S0045-6535(03)00038-9)
- Paraskos, J., Frayer, J., & Shah, Y. (1975). Effect of holdup incomplete catalyst wetting and backmixing during hydroprocessing in trickle bed reactors. *Industrial & Engineering Chemistry Process Design and Development*, 14(3), 315-322. <https://doi.org/10.1021/i260055a021>
- Peyton, B. M., Wilson, T., & Yonge, D. R. (2002). Kinetics of phenol biodegradation in high salt solutions. *Water research*, 36(19), 4811-4820. [https://doi.org/10.1016/S0043-1354\(02\)00200-2](https://doi.org/10.1016/S0043-1354(02)00200-2)
- Piccinin, L. d. G. (2022). Catalytic application of carbon nanotubes obtained from plastic solid waste in the removal of quinoline from isooctane by selective oxidation with hydrogen peroxide. *Thesis.Universidade Tecnológica Federal do Parana*. <https://hdl.handle.net/10198/25583>
- Rueda Márquez, J. J., Levchuk, I., & Sillanpää, M. (2018). Application of catalytic wet peroxide oxidation for industrial and urban wastewater treatment: A review. *Catalysts*, 8(12), 673. <https://doi.org/10.3390/catal8120673>
- Sachdeva, T., & Pant, K. (2010). Deep desulfurization of diesel via peroxide oxidation using phosphotungstic acid as phase transfer catalyst. *Fuel processing technology*, 91(9), 1133-1138. <https://doi.org/10.1016/j.fuproc.2010.03.027>

- Saha, B., Kumar, S., & Sengupta, S. (2019). Green synthesis of nano silver on TiO<sub>2</sub> catalyst for application in oxidation of thiophene. *Chemical Engineering Science*, 199, 332-341. <https://doi.org/10.1016/j.ces.2018.12.063>
- Saravanan, A., Kumar, P. S., Jeevanantham, S., Karishma, S., Tajsabreen, B., Yaashikaa, P., & Reshma, B. (2021). Effective water/wastewater treatment methodologies for toxic pollutants removal: Processes and applications towards sustainable development. *Chemosphere*, 280, 130595. <https://doi.org/10.1016/j.chemosphere.2021.130595>
- Shahidi, D., Roy, R., & Azzouz, A. (2015). Advances in catalytic oxidation of organic pollutants—prospects for thorough mineralization by natural clay catalysts. *Applied Catalysis B: Environmental*, 174, 277-292. <https://doi.org/10.1016/j.apcatb.2015.02.042>
- Stefanakis, A. I., & Thullner, M. (2016). Fate of phenolic compounds in constructed wetlands treating contaminated water. *Phytoremediation: Management of Environmental Contaminants, Volume 4*, 311-325. [https://doi.org/10.1007/978-3-319-41811-7\\_16](https://doi.org/10.1007/978-3-319-41811-7_16)
- Wang, K., Han, C., Shao, Z., Qiu, J., Wang, S., & Liu, S. (2021). Perovskite oxide catalysts for advanced oxidation reactions. *Advanced Functional Materials*, 31(30), 2102089. <https://doi.org/10.1002/adfm.202102089>
- Wang, P., Bian, X., & Li, Y. (2012). Catalytic oxidation of phenol in wastewater—A new application of the amorphous Fe<sub>78</sub>Si<sub>9</sub>B<sub>13</sub> alloy. *Chinese Science Bulletin*, 57(1), 33-40. <https://doi.org/10.1007/s11434-011-4876-2>
- Xu, Q., Siracusa, G., Di Gregorio, S., & Yuan, Q. (2018). COD removal from biologically stabilized landfill leachate using Advanced Oxidation Processes (AOPs). *Process Safety and Environmental Protection*, 120, 278-285. <https://doi.org/10.1016/j.psep.2018.09.014>
- Yan, Y., Wu, X., & Zhang, H. (2016). Catalytic wet peroxide oxidation of phenol over Fe<sub>2</sub>O<sub>3</sub>/MCM-41 in a fixed bed reactor. *Separation and Purification Technology*, 171, 52-61. <https://doi.org/10.1016/j.seppur.2016.06.047>
- Yaqub, A., Isa, M. H., Ajab, H., & Junaid, M. (2017). Preparation of Ti/TiO<sub>2</sub> Anode for Electrochemical Oxidation of Toxic Priority Pollutants. *Journal of New Materials for Electrochemical Systems*, 20(1). <https://doi.org/10.14447/jnmes.v20i1.287>
- Zazo, J. A., Pliego, G., Blasco, S., Casas, J. A., & Rodriguez, J. J. (2011). Intensification of the Fenton process by increasing the temperature. *Industrial & Engineering Chemistry Research*, 50(2), 866-870. <https://doi.org/10.1021/ie101963k>



© 2023. The Author(s). This article is an open access article distributed under the terms and conditions of the Creative Commons Attribution-ShareAlike 4.0 (CC BY-SA) International License (<http://creativecommons.org/licenses/by-sa/4.0/>)